Supporting Information for

Estimating diurnal courses of gross primary production for maize: a comparison of sun-induced chlorophyll fluorescence, light-use efficiency and process-based models

Tianxiang Cui [1,2], Rui Sun [1,2,*], Chen Qiao [1,2], Qiang Zhang [1,2], Tao Yu [1,2], Gang Liu [1,2] and Zhigang Liu [1,2]

[1] State Key Laboratory of Remote Sensing Science, Jointly Sponsored by Beijing Normal University and Institute of Remote Sensing and Digital Earth of Chinese Academy of Sciences, Beijing 100875, China; txiang.c@gmail.com (T.C.); qiaochenbnu@gmail.com (C.Q.); zhangqiang1228@mail.bnu.edu.cn (Q.Z.); yutaogis@163.com (T.Y.); 1015220446@qq.com (G.L.); zhigangliu@bnu.edu.cn (Z.L)

[2] Beijing Engineering Research Center for Global Land Remote Sensing Products, Institute of Remote Sensing Science and Engineering, Faculty of Geographical Science, Beijing Normal University, Beijing 100875, China

***** Correspondence: sunrui@bnu.edu.cn; Tel.: +86-10-5880-5457

Introduction

This supporting file provides a more detailed description of the method to determining water stress factor in the MuSyQ-GPP algorithm and results obtained using SIF686.

Text S1. Estimation of water stress factor in the MuSyQ-GPP algorithm

The limited effect of water conditions on plant photosynthesis, ranging between 0.5 and 1, is derived following the algorithm

$$f_2(\beta)=0.5+0.5E/E_{\mathrm{P}} \quad (1)$$

where E and E_P represent actual and potential evapotranspiration, respectively.

In the MuSyQ-GPP algorithm, a modified Penman-Monteith (P-M) approach with biome-specific canopy conductance was used to estimate actual evapotranspiration (Qiao et al. 2015; Zhang et al. 2009). The available energy component for canopy (A_{canopy}) and soil (A_{soil}) are generated using FPAR

$$A_{canopy} = FPAR \times A \tag{2}$$

$$A_{soil} = (1 - FPAR) \times A \tag{3}$$

where A is approximated as net radiation consisting both net shortwave radiation and net longwave radiation. Vegetation transpiration is defined as

$$\lambda E_{canopy} = \frac{\Delta A_{canopy} + \rho C_p VPD g_a}{\Delta + \gamma(1 + g_a / g_c)} \tag{4}$$

where λE_{canopy} (W m^{-2}) is the latent heat flux of canopy, $\triangle = d(e_{sat})/dT$ (Pa K^{-1}) is the slope of the curve relating saturated water vapor pressure e_{sat} (Pa) to air temperature T (K), ρ (kg m^{-3}) is air density, C_p (J kg^{-1} K^{-1}) is the specific heat of air at constant pressure, $VPD = e_{sat} - e$ (Pa) is the vapor pressure deficit of air, g_a (m s^{-1}) is aerodynamic conductance and defined as 0.01 m s^{-1} in our study by referring to Zhang et al. (2008), γ (Pa k^{-1}) is psychometric constant, and g_c (m s^{-1}) is canopy conductance and can be described as

$$g_c = \frac{g_{sx}}{K_Q} \ln\left[\frac{Q_h + Q_{50}}{Q_h \exp(-K_Q LAI) + Q_{50}}\right]\left[\frac{1}{1 + VPD/D_{50}}\right] \tag{5}$$

where K_Q is the extinction coefficient for PAR, Q_h is the PAR at the top of canopy, Q_{50} and D_{50} are the values of APAR and water vapor deficit when stomatal conductance is half its maximum value, respectively. For our study, values of g_{sx}, K_Q and D_{50} are assigned to 0.0032 m s^{-1}, 0.6 and 800 Pa, respectively (Zhang et al., 2008).

Soil evaporation is calculated using a soil evaporation equation (Mu et al. 2011; Zhang et al. 2009):

$$\lambda E_{soil} = RH^{(VPD/k)} \frac{\Delta A_{soil} + \rho C_p VPD g_a}{\Delta + \gamma \times g_a / g_{totc}} \tag{6}$$

where λE_{soil} (W m^{-2}) is the latent heat flux of soil, RH is the relative humidity of air with values ranging from 0 to 1, k (Pa) is a parameter to fit the complementary relationship and is empirically adjusted for different vegetation types, and g_{totc} (m s^{-1}) is the corrected value of total aerodynamic conductance as described by Zhang et al. (2010).

The potential evapotranspiration, E_P, is calculated using the Priestley and Taylor (P-T) equation (Priestley and Taylor, 1972).

$$\lambda E_p = \varphi A \frac{\Delta}{\Delta + \gamma} \tag{7}$$

where the P-T coefficient φ was set to 1.26 following Priestley and Taylor (1972) in the study.

Text S2. Performance of the SIF_{686}-based GPP model

SIF_{686} was less correlated with GPP than SIF_{760}. The optical absorption at far-red band of a leaf is smaller than 10%, while it is over 90% at the red band (Jacquemoud and Baret, 1990). The reabsorption of SIF_{686} influenced by chlorophyll content and canopy structure is larger than that of SIF_{760} (Liu et al. 2016, 2017). Therefore, SIF_{686} values presented a larger diversity than SIF_{760} at the four positions of the canopy and the SIF_{686}-based GPP model showed a much limited performance than SIF_{760}.

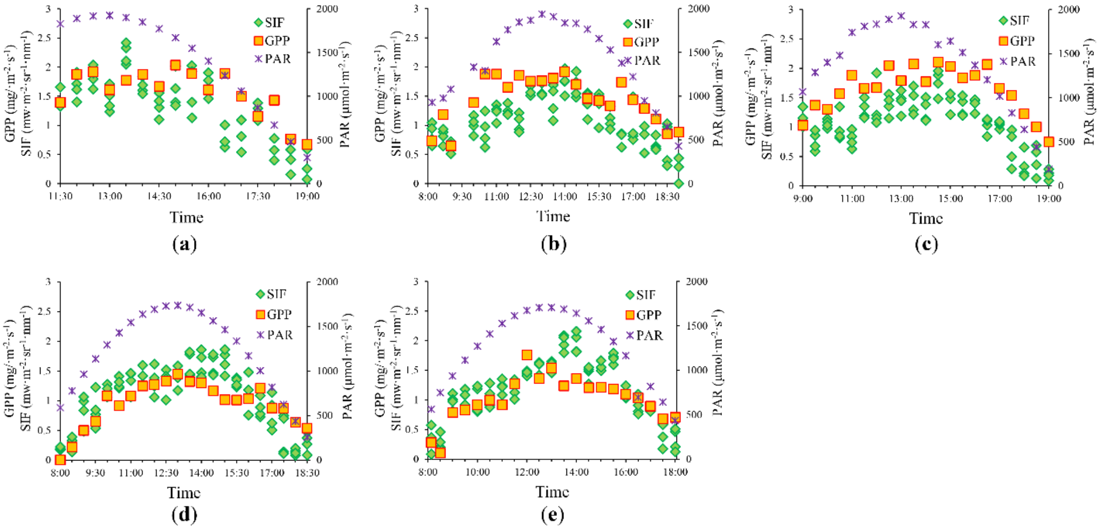

Figure S1. Diurnal patterns of PAR, GPP and SIF_{686} during the experiment: (**a**) July 10th. (**b**) July 17th. (**c**) July 18th. (**d**) August 21st. (**e**) August 22nd.

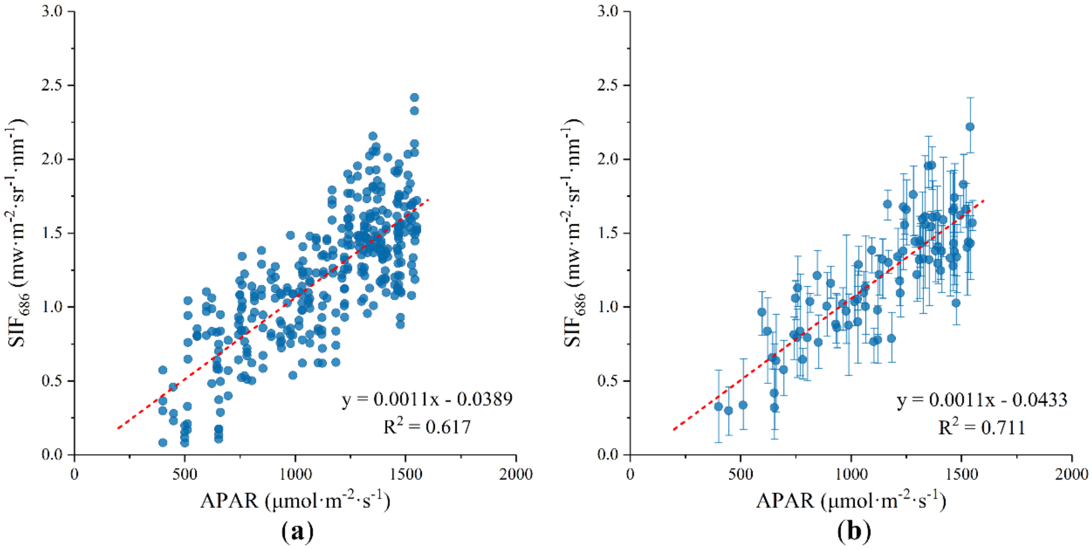

Figure S2. Relationship between APAR and (**a**) individual SIF_{686} and (**b**) averaged SIF_{686}. The error bar indicates the range of SIF_{686} values for four measurements.

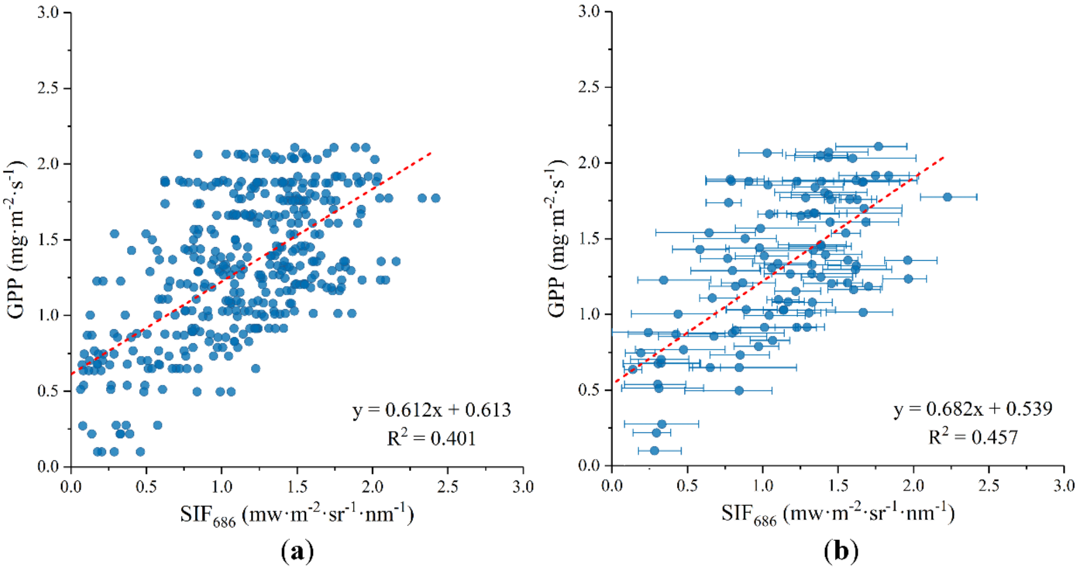

Figure S3. Relationship between (**a**) individual SIF_{686} and GPP, (**b**) averaged SIF_{686} and GPP. The error bars indicate the range of SIF_{686} values for the four measurements.

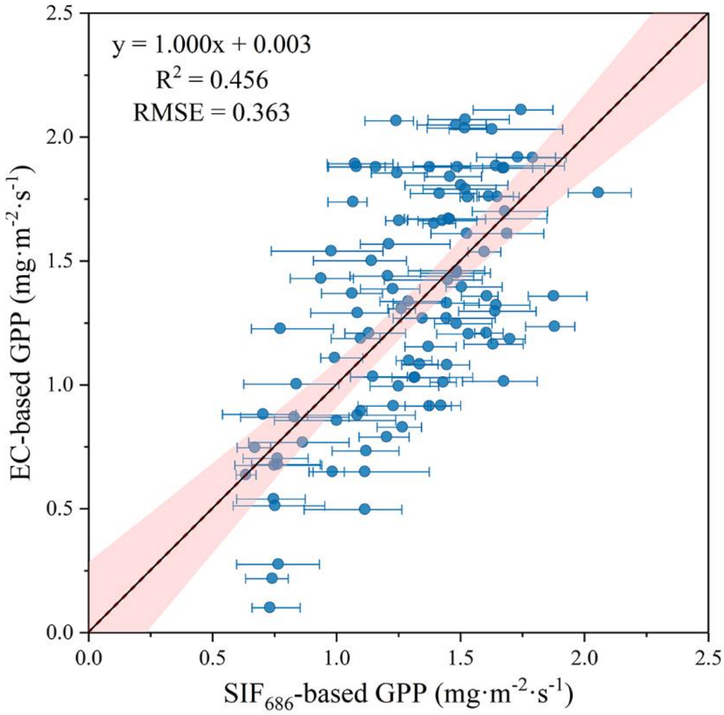

Figure S4. Relationships between SIF_{686}-based GPP and EC-based GPP during the experiment period. The red shades represent the 95% confidence bands for the regression functions.

References

Mu, Q.Z., Zhao, M.S., Running, S.W., 2011. Improvements to a MODIS global terrestrial evapotranspiration algorithm. Remote Sensing of Environment, 115, 1781-1800. https://doi.org/10.1016/j.rse.2011.02.019.

Priestley, C.H.B., Taylor, R.J., 1972. On the assessment of surface heat flux and evaporation using large-scale parameters. Monthly weather review, 100, 81-92. https://doi.org/10.1175/1520-0493(1972)100<0081:otaosh>2.3.co;2.

Qiao, C., Sun, R., Xu, Z.W., Zhang, L., Liu, L.Y., Hao, L.Y., Jiang, G.Q., 2015. A Study of Shelterbelt Transpiration and Cropland Evapotranspiration in an Irrigated Area in the Middle Reaches of the Heihe River in Northwestern China. IEEE Geoscience and Remote Sensing Letters, 12, 369-373.

https://doi.org/10.1109/lgrs.2014.2342219.

Zhang, K., Kimball, J.S., Mu, Q.Z., Jones, L.A., Goetz, S.J., Running, S.W., 2009. Satellite based analysis of northern ET trends and associated changes in the regional water balance from 1983 to 2005. Journal of Hydrology, 379, 92-110. https://doi.org/10.1016/j.jhydrol.2009.09.047.

Zhang, K., Kimball, J.S., Nemani, R.R., Running, S.W., 2010. A continuous satellite-derived global record of land surface evapotranspiration from 1983 to 2006. Water Resources Research, 46. https://doi.org/10.1029/2009wr008800.

Zhang, Y.Q., Chiew, F.H.S., Zhang, L., Leuning, R., Cleugh, H.A., 2008. Estimating catchment evaporation and runoff using MODIS leaf area index and the Penman-Monteith equation. Water Resources Research, 44. https://doi.org/10.1029/2007wr006563.

Jacquemoud, S., Baret, F. 1990. PROSPECT: A Model of Leaf Optical Propertiesspectra. Remote Sensing of Environment, 34: 75–91. https://doi.org/0034-4257(90)90100-Z.

Liu, L.Y., Liu, X.J., Guan, L.L. 2016. Uncertainties in linking solar-induced chlorophyll fluorescence to plant photosynthetic activities. Geoscience and Remote Sensing Symposium (IGARSS), 2016 IEEE International, 4414-4417.

Liu, L.Y., Liu, X.J., Hu, J.C., Guan, L.L. 2017. Assessing the wavelength-dependent ability of solar-induced chlorophyll fluorescence to estimate the GPP of winter wheat at the canopy level. International Journal of Remote Sensing, 38: 4396-4417. http://dx.doi.org/10.1080/01431161.2017.1320449